

Soliton propagation in an erbium-doped fiber with and without a continuous wave backgroundR. Ganapathy,^{1,*} V. C. Kuriakose,^{1,†} and K. Porsezian^{2,‡}¹*Department of Physics, Cochin University of Science and Technology, Kochi 682 022, India*²*Raman School of Physics, Pondicherry University, R. V. Nagar, Pondicherry 605 014, India*

(Received 9 April 2003; published 31 December 2003)

Considering ultrashort pulse propagation in a nonlinear resonant fiber governed by Hirota-Maxwell Bloch equations, the soliton interaction in an erbium-doped fiber system associated with higher-order dispersion, self-steepening, and self-induced transparency effects is studied for the case when the fiber is driven with and without a constant pumping source. Using auto-Bäcklund-transformation, one- and two-soliton solutions are generated. The significance of the results is discussed in detail.

DOI: 10.1103/PhysRevE.68.066615

PACS number(s): 42.81.Dp, 02.30.Ik, 42.65.Tg

I. INTRODUCTION

The field of optical solitons has considerable potential for ultrafast technological applications, and it presents many exciting research problems both from fundamental and applied points of view [1]. Solitons are envisaged by communication experts all over the world as the future tools in achieving the endeavor of an ideal global village where information travels very fast and communication is efficient and cost effective. Experiments done at different laboratories have confirmed the theoretical conjecture about the feasibility of ultrafast, long-distance, and less expensive communication systems without any loss of power using optical solitons as bits of information. In the last decade, many distinguished physicists, applied mathematicians, and engineers have contributed in a major way to this exciting area of research. Optical communication is a wonderful example of how the interplay between mathematics and more applied research has generated significant technological advances. Many technological applications of optical solitons are being actively pursued, including soliton switching, pulse compression, dispersion management, wavelength conversion, and so on [1–8].

The propagation of temporal soliton envelopes in nonlinear optical media has been predicted and demonstrated experimentally. This prediction arises from the opportunity of reducing the Maxwell equations, which govern the propagation to a single completely integrable soliton equation in the form of nonlinear Schrödinger (NLS) equation. Soliton-type pulse propagation through nonlinear optical fibers is realized by means of the exact counterbalance between the major constraints of the fiber, viz., group velocity dispersion which broadens the pulse and the self-phase modulation which contracts the pulse. The propagation of optical pulses through a nonlinear fiber in the picosecond regime is described by the well-known NLS equation. With the current interest of using solitons as pulse bits in long optical fibers for communication purposes, it is important for us to reevaluate the practicality of using analytical techniques for predicting the behavior of such bits. Since such pulses are near a pure soliton

solution, it becomes feasible to use analytical soliton techniques and potentiality of obtaining useful analytical results becomes very high. In order to increase the bit rates, it is necessary to decrease the pulse width. As pulse lengths become comparable to the wavelength, however, the NLS equation becomes inadequate, additional terms have to be included, and the resulting pulse propagation is called as higher-order nonlinear Schrödinger (HNLS) equation which is of the form [1,2,5,6,9,10]

$$iu_{\zeta} + \frac{1}{2}u_{\tau\tau} + |u|^2u + i\varepsilon[\beta_1u_{\tau\tau\tau} + \beta_2(|u|^2u)_{\tau} + (\beta_3 + i\sigma_R)u(|u|^2)_{\tau}] = 0. \quad (1)$$

u denotes the normalized slowly varying complex pulse envelope, τ is the normalized retarded time in the nondimensional form and ζ is the normalized propagation distance also in the non-dimensional form. The perturbation term ε is the relative spectral width. Equation (1) includes effects such as third-order dispersion (term corresponding to β_1), self-steepening (term corresponding to β_2), and stimulated Raman scattering (term corresponding to $\beta_3 + i\sigma_R$). All the coefficients in the higher-order terms are real. The terms with β_1 , β_2 , and β_3 give perturbations of dispersive or Hamiltonian type and the resulting equation has been thoroughly analyzed by Kodama [11,13]. The term with σ_R corresponds to self-induced Raman effect. It is well known that the third-order dispersion (TOD) effect is responsible for splitting-up of higher-order solitons. The inelastic Raman scattering is due to the delayed response of the medium which forces the pulse to undergo a frequency shift and known as self-frequency shift. The effect of self-steepening is due to the intensity-dependent group velocity of the optical pulse, which gives the pulse a very narrow width in the course of propagation. Because of this, the peak of the pulse will travel slower than the wings. Among the effects associated with third-order nonlinearity, stimulated Raman scattering and stimulated Brillouin scattering limit the maximum input power available for transmission, whereas self-phase modulation directly influences the dispersion by modifying the pulse shape and thus can play a vital role, together with chromatic dispersion, in determining the transmission rate attainable in a given fiber.

*Electronic address: ganapathy@eth.net

†Electronic address: vck@cusat.ac.in

‡Electronic address: ponzsol@yahoo.com

Equation (1) is found to be integrable for the case $\sigma_R = 0$, $\beta_1 = 1$, $\beta_2 = 6$, and $\beta_3 = -3$ for which multisoliton solutions have been obtained using inverse scattering transform [12]. In Ref. [13], when $\sigma_R = 0$, employing a certain Lie transformation from the perturbed equation, Kodama was able to reduce Eq. (1) to an integrable form by considering terms up to $O(\varepsilon)$ only leading to the Hirota equation given by

$$iu_\zeta + \frac{1}{2}u_{\tau\tau} + |u|^2u + i\varepsilon\beta_1(u_{\tau\tau\tau} + 6|u|^2u_\tau) = 0, \quad (2)$$

for which Hirota had already obtained multisoliton solutions using the inverse scattering transform [14].

The propagation of the optical solitons that we have discussed so far results from compensation between self-phase-modulation and group-velocity dispersion and other higher-order effects. A different type of optical soliton is associated with the self-induced transparency (SIT) effect in resonant absorbers. In 1967, McCall and Hahn have proposed SIT soliton in two-level resonant atoms [3].

In theoretical description of this strongly resonant situation it is frequently possible to ignore all other energy levels of the atoms and treat the interaction of light with a so-called two-level atom. By assuming classical treatment of light, resonant interaction of intense light with matter can be treated quite thoroughly. Extensive investigation of this strongly resonant situation led to the observation of soliton behavior, both in experiments and in numerical solutions of the governing equations [15,16]. SIT equations are frequently referred to as the Maxwell-Bloch (MB) equations. Lamb gave an elaborate study on different limiting cases of the MB equations [4]. The connection between MB equations and the sine-Gordon equation is explained in literature [10]. Owing to the large enhancement of the nonlinearity in resonant media, which is not accompanied here by absorption as occurs in the CW case, it is clear that guided SIT solitons are potentially very attractive for applications involving both low power and ultrafast all-optical signal processing [17,18].

When Er is doped with the core of the optical fibers, then the nonlinear wave propagation can have both the effects due to silica and Er impurities. Er impurities give SIT effect to the optical pulse whereas the silica material gives the NLS soliton effect [17–19,21–24]. Thus the important constraint to the NLS soliton, namely, the optical losses can be somewhat compensated with the effect of SIT. So if we consider these effects for a large width pulse then the system dynamics will be governed by the coupled system of the NLS equation and the MB equation (NLS-MB system). Maimistov *et al.*, in 1983, proposed the system and obtained the Lax pair and the inverse scattering technique (IST) for the soliton solution [7].

Porsezian and Nakkeeran also proved the coexistence of the NLS soliton and the MB soliton and also established the Painlevé property [23]. Doktorov and Vlasov gave a good explanation to the possibility of the NLS-MB solitons [19]. Kakei and Satsuma derived the N -soliton solution for the NLS-MB equations using the IST [22].

Nakazawa *et al.* reported that a stable $2\pi/N=1$, NLS-MB soliton exists [17,18]. Also, the multiple-soliton structure proved that the higher-order NLS-MB solitons always split into multiple $(2\pi/N)=1$ solitons. These properties are also confirmed through a computer run. The phase change of the new soliton is governed solely by the NLS component, while the pulse delay is determined solely by the SIT component when the detuning from the resonance is zero. The propagation and switching of SIT in nonlinear directional couplers with a two-level atom has been recently investigated numerically by retaining the transverse dependence of the optical field and atomic variables. This work demonstrated that the self-confinement due to the guiding structure permits the injected SIT soliton to maintain its particlelike behavior. Recent experiments by Nakazawa *et al.* have confirmed guided wave SIT soliton formation and propagation by employing a few meters of erbium-doped fiber, which was cooled to 4.2 K [17,18]. This justifies the approximation of treating ultrashort pulse propagation in waveguide or fiber couplers doped with resonant two-level centres. To the best of our knowledge, only a small number of works have been reported for the higher-order effects with SIT effects.

The prime aim of this paper is to consider the impact of higher-order perturbation terms appearing in Eq. (2) and to generate the two-soliton solutions of the Hirota-MB equations with and without the pumping effect. The paper is outlined as follows. In Sec. II the theoretical formulation of the problem is presented. In Sec. III, considering the linear eigenvalue problem and the auto-Bäcklund-transformation method, single- and two-soliton solutions for the vacuum soliton case as well as that for the constant pumping source case are presented. In Sec. IV, the conclusions are made.

II. THEORETICAL MODEL

As in a pure silica fiber, under the influence of ultrashort pulse propagation Er doped fiber also suffers from the higher-order effects such as TOD, self-steepening (SS), and stimulated Raman scattering (SRS). Nakkeeran and Porsezian, in their work, have included all these effects by considering the coupled system of HNLS-MB equations which are integrable only for certain parametric choices [24] and have obtained one soliton solution by employing an auto-Bäcklund-transformation resulting from a 3×3 Lax pair in addition to group velocity dispersion (GVD) and self-phase modulation (SPM) effects. Doktorov and Vlasov also considered the SS effect and showed that the coupled system of derivative nonlinear Schrödinger-Maxwell Bloch fiber system allows soliton type pulse propagation [20]. From the literature, it is also established that the influence of additional effects such as TOD and SS on the NLS soliton results in splitting of the bound soliton state due to the difference in speed of each of the solitons and also due to modifications in the velocity components. By considering the higher-order perturbation terms appearing in Eq. (2), Porsezian and Nakkeeran proposed the coupled system of the Hirota and the MB equation (H-MB system) recently, which governs the wave propagation of ultrashort pulses (USP) in Er-doped fibers. The H-MB system equation is given by [23]

$$iu_\zeta + \frac{1}{2}u_{\tau\tau} + |u|^2u + i\varepsilon\beta_1(u_{\tau\tau\tau} + 6|u|^2u_\tau) + \langle p \rangle = 0, \quad (3)$$

$$p_\tau - 2i(\omega p + \eta u) = 0,$$

$$\eta_\tau - i(pu^* - up^*) = 0,$$

where $\langle \dots \rangle$ is the averaging function over the entire frequency range. For example,

$$\langle p(\zeta, \tau; \omega) \rangle = \int_{-\infty}^{+\infty} p(\zeta, \tau; \omega) g(\omega) d\omega, \quad (4)$$

such that

$$\int_{-\infty}^{+\infty} g(\omega) d\omega = 1. \quad (5)$$

$g(\omega)$ is the distribution function which represents the uncertainty in the energy level of the resonant atoms. p is a measure of the polarization of the resonant medium and η denotes the extent of population inversion. In an earlier work, Porsezian and Nakkeeran [23], have constructed only one soliton solution for Eq. (3), but have not analyzed the interaction scenario and the concept of continuous wave background, which are the main results in this paper.

III. SOLITON SOLUTIONS

In Ref. [23], Porsezian and Nakkeeran analyzed the possibility of soliton pulse propagation using Painlevé analysis and constructed the Lax-pair and one-soliton solution through Bäcklund transformation [23,24]. As our main aim in this paper is to generate two soliton solutions, in the following, we use the auto-Bäcklund-transformation method and generate soliton solutions with and without continuous wave background. For this purpose, we consider the linear eigenvalue problem for Eq. (3), which is of the form

$$\begin{aligned} \psi_\tau &= Q_1 \psi, \\ \psi_\zeta &= Q_2 \psi, \\ \psi &= (\psi_1, \psi_2)^T, \end{aligned} \quad (6)$$

where

$$Q_1 = \begin{pmatrix} -i\lambda & u \\ -u^* & i\lambda \end{pmatrix} \quad (7)$$

and

$$Q_2 = \begin{pmatrix} A & B \\ C & -A \end{pmatrix} \quad (8)$$

with

$$\begin{aligned} A &= -i\lambda^2 + \frac{i}{2}|u|^2 + \varepsilon\beta_1(-4i\lambda^3 + 2i\lambda|u|^2 + uu_\tau^* - u^*u_\tau) \\ &\quad - \left\langle \frac{i\eta}{2(\lambda + \omega)} \right\rangle, \end{aligned} \quad (9)$$

$$\begin{aligned} B &= \lambda u + \frac{i}{2}u_\tau + \varepsilon\beta_1(4\lambda^2u + 2i\lambda u_\tau - 2|u|^2u - u_{\tau\tau}) \\ &\quad + \left\langle \frac{p}{2(\lambda + \omega)} \right\rangle, \end{aligned}$$

$$\begin{aligned} C &= -\lambda u^* + \frac{i}{2}u_\tau^* + \varepsilon\beta_1(-4\lambda^2u^* + 2i\lambda u_\tau^* + 2|u|^2u^* + u_{\tau\tau}^*) \\ &\quad - \left\langle \frac{p^*}{2(\lambda + \omega)} \right\rangle, \end{aligned}$$

such that $Q_{1\zeta} - Q_{2\tau} + [Q_1, Q_2] = 0$ gives back Eq. (3). From the linear eigen value problem given by Eq. (6), soliton solutions are generated for Eq. (3) using auto-Bäcklund-transformation technique and thereby the recurrence relations connecting the n th (primed) and $(n-1)$ th (unprimed) soliton wave functions are obtained in the form

$$\begin{aligned} \psi'_1 &= (-i\lambda + i\mu' - \frac{1}{2}\sqrt{4\nu'^2 - |u+u'|^2})\psi_1 + \frac{1}{2}(u+u')\psi_2, \\ \psi'_2 &= -\frac{1}{2}(u^*+u'^*)\psi_1 + (i\lambda - i\mu' - \frac{1}{2}\sqrt{4\nu'^2 - |u+u'|^2})\psi_2, \end{aligned} \quad (10)$$

where μ' and ν' are real constants denoting the soliton velocity and amplitude parameters, respectively, and $\lambda \equiv \mu' + i\nu'$. The recurrence relation connecting the n th (primed) and $(n-1)$ th (unprimed) soliton solutions is of the form

$$u+u' = \frac{-4\Gamma\nu'}{1+|\Gamma|^2}, \quad (11)$$

where $\Gamma = \psi_1/\psi_2$. Moreover, $u' \equiv u(n)$ and $u \equiv u(n-1)$, $n = 1, 2, \dots$ such that $u(1)$ refers to the one-soliton solution and so on.

Now two different cases are considered (i) vacuum soliton case for which $u(0) = 0$ is taken as the seed solution and (ii) $u(0) = \kappa$, which represents a constant pumping source and is complex.

A. Vacuum soliton case

Here we assume $u(0) = 0$. Hence from Eqs. (6) and (7), and with the condition for the pure state given by $p = 0$ [23,24] and $\eta = 1$, the relation between the wave functions is given by

$$\begin{aligned} \psi_1(0) &= c_1(0)\exp(A\zeta - i\lambda\tau), \\ \psi_2(0) &= c_2(0)\exp[-(A\zeta - i\lambda\tau)], \end{aligned} \quad (12)$$

where $c_i(0)$ ($i=1,2$) are integration constants. The pseudospectral function $\Gamma(0)$ is given by

$$\Gamma(0) \equiv \frac{\psi_1(0)}{\psi_2(0)} = C(0)\exp[2(A\zeta - i\lambda\tau)], \quad (13)$$

where $C(0) \equiv c_1(0)/c_2(0)$. On substituting these in Eq. (11), the one-soliton solution is obtained as

$$\begin{aligned}
 u(\zeta, \tau) &\equiv u(1) \\
 &= -2\nu(1)\text{sech}\{2[(A_{11}+Av_1)\zeta + \nu(1)\tau \\
 &\quad + \nu(1)\Delta_1]\}\exp\{-2i[(A_{12}+Av_2)\zeta \\
 &\quad + \mu(1)\tau + \delta_1]\}, \tag{14}
 \end{aligned}$$

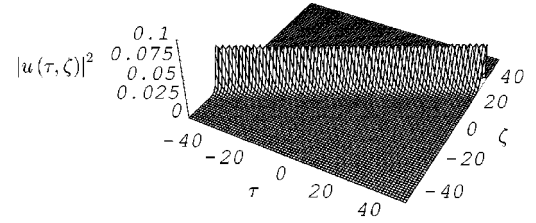
where δ_1 and Δ_1 are integration phase constants and the other parameters are given by

$$A_{11} = 2\mu(1)\nu(1) + 4\varepsilon\beta_1[3\mu^2(1)\nu(1) - \nu^3(1)],$$

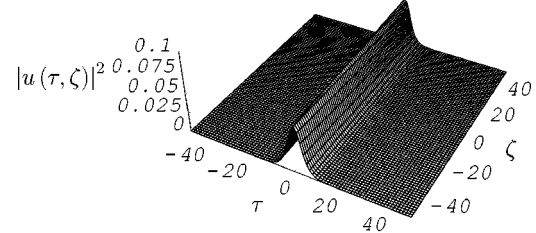
$$A_{12} = 4\varepsilon\beta_1\{\mu(1)[\mu^2(1) - 3\nu^2(1)]\} + [\mu^2(1) - \nu^2(1)],$$

$$\begin{aligned}
 Av_1 &= \left\langle \frac{\nu(1)}{2\{[\mu(1) + \omega]^2 + \nu^2(1)\}} \right\rangle, \\
 Av_2 &= \left\langle \frac{(\mu(1) + \omega)}{2\{[\mu(1) + \omega]^2 + \nu^2(1)\}} \right\rangle. \tag{15}
 \end{aligned}$$

Figure 1(a) shows the surface plot of $|u(\zeta, \tau)|^2$ when $g(\omega)$ given by Eq. (5) takes the form of a Dirac delta function $\delta(\omega - \omega_0)$ at the resonant frequency ω_0 . Hence from Eq. (4), $\langle p(\zeta, \tau; \omega) \rangle = p(\zeta, \tau; \omega_0)$. It is clear from Fig. 1 that $p(\zeta, \tau; \omega_0)$ is responsible for introducing a phase shift from that of the ordinary nonlinear Schrödinger equation case as shown in Fig. 1(b). On substituting Eq. (14) into Eq. (3), the corresponding measure of the polarization of the resonant medium denoted by p and the extent of population inversion denoted by η can be readily obtained having the respective expressions



(a)



(b)

FIG. 1. (a) Surface plot of the intensity of the soliton solution given by Eq. (14) when $g(\omega) = \delta(\omega - \omega_0)$, where the resonant frequency $\omega_0 = 0.5$. (b) Surface plot of the intensity of the soliton solution for the ordinary nonlinear Schrödinger equation.

$$\begin{aligned}
 p(\zeta, \tau) &= \nu(1)\text{sech}(a\zeta + b\tau + c)[2f_1 - f_2^2(1 + 2f_2) \\
 &\quad - 2i[a - bf_2(1 + 3f_2)]\tanh(a\zeta + b\tau + c) \\
 &\quad + b^2(1 + 6f_2)\tanh^2(a\zeta + b\tau + c) - 2ib^3\tanh^3 \\
 &\quad \times (a\zeta + b\tau + c) + \text{sech}^2(a\zeta + b\tau + c)(-\{(1 + 6f_2) \\
 &\quad \times [b^2 - 8\nu^2(1)]\} + 2ib[5b^2 - 24\nu^2(1)] \\
 &\quad \times \tanh(a\zeta + b\tau + c))\exp(f_1\zeta + f_2\tau + f_3) \tag{16}
 \end{aligned}$$

and

$$\begin{aligned}
 \eta(\zeta, \tau) &= \frac{1}{4}(2b^2[24\nu^2(1) - 5b^2]\text{sech}^4(a\zeta + b\tau + c) + \text{sech}^2(a\zeta + b\tau + c)\{2ab - 3b^2f_2(1 + 4f_2) + (1 + 6f_2) \\
 &\quad \times [8f_2\nu^2(1) + 16\omega_0\nu^2(1) - 2b^2\omega_0] + ib(1 + 8f_2 + 4\omega_0)[5b^2 - 24\nu^2(1)]\tanh(a\zeta + b\tau + c) + 36b^2 \\
 &\quad \times [b^2 - 4\nu^2(1)]\tanh^2(a\zeta + b\tau + c)\} + [f_2 + 2\omega_0 - ib \tanh(a\zeta + b\tau + c)]\{2f_1 - f_2^2(1 + 2f_2) - 2i[a - bf_2(1 + 3f_2)] \\
 &\quad \times \tanh(a\zeta + b\tau + c) + b^2(1 + 6f_2)\tanh^2(a\zeta + b\tau + c) - 2ib^3\tanh^3(a\zeta + b\tau + c)\}, \tag{17}
 \end{aligned}$$

where

$$\begin{aligned}
 a &= 2(A_{11} + Av_1), \quad b = 2\nu(1), \quad c = 2\nu(1)\Delta_1, \\
 f_1 &= 2(A_{12} + Av_2), \quad f_2 = 2\mu(1), \quad f_3 = 2\delta_1.
 \end{aligned}$$

Once again on using the recurrence relations given by Eq. (10), the two-soliton solution for Eq. (3) is obtained and is of the form

$$u(2) \equiv u_2(\zeta, \tau) = \frac{N(\zeta, \tau)}{D(\zeta, \tau)}, \tag{18}$$

where

$$\begin{aligned}
 N(\zeta, \tau) &= 2\nu(1)\text{sech}(\xi_1)\exp(-i\chi_1)(\Delta\mu)^2 \\
 &\quad + 4i\nu(1)\text{sech}(\xi_1)\exp(-i\chi_1)\nu(2)\Delta\mu \tanh(\xi_2) \\
 &\quad + 2\nu(1)\text{sech}(\xi_1)\exp(-i\chi_1)[\nu^2(1) - \nu^2(2)] \\
 &\quad + 2\nu(2)\text{sech}(\xi_2)\exp(-i\chi_2)(\Delta\mu)^2 \\
 &\quad - 4i\nu(2)\text{sech}(\xi_2)\exp(-i\chi_2)\nu(1)\Delta\mu \tanh(\xi_1) \\
 &\quad - 2\nu(2)\text{sech}(\xi_2)\exp(-i\chi_2)[\nu^2(1) - \nu^2(2)],
 \end{aligned}$$

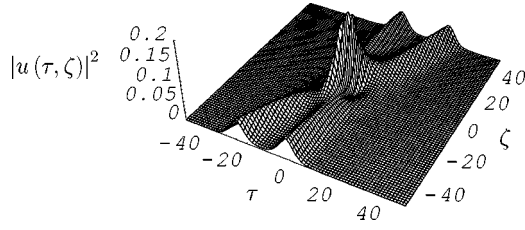


FIG. 2. Surface plot of the in-phase injection of the two soliton solution given by Eqs. (18), (19), and (20) when $g(\omega) = \delta(\omega - \omega_0)$, where the resonant frequency $\omega_0 = 0.5$.

$$\begin{aligned}
 D(\zeta, \tau) = & (\Delta\mu)^2 + \nu^2(1) + \nu^2(2) \\
 & - 2\nu(1)\nu(2)\tanh(\xi_1)\tanh(\xi_2) \\
 & - 2\nu(1)\nu(2)\text{sech}(\xi_1)\text{sech}(\xi_2)\cos(\chi_2 - \chi_1)
 \end{aligned} \quad (19)$$

with

$$\begin{aligned}
 \xi_i = & 2 \left(2\mu(i)\nu(i) - \frac{\nu(i)}{2[(\mu(i) + \omega_0)^2 + \nu^2(i)]} \right. \\
 & \left. + 4\varepsilon\beta_1[3\mu^2(i)\nu(i) - \nu^3(i)] \right) \zeta + 2[\nu(i)\tau + \nu(i)\Delta_i], \\
 \chi_i = & 2 \left(\mu^2(i) - \nu^2(i) + \frac{[\mu(i) + \omega_0]}{2[(\mu(i) + \omega_0)^2 + \nu^2(i)]} \right. \\
 & \left. + 4\varepsilon\beta_1[\mu^3(i) - 3\mu(i)\nu^2(i)] \right) \zeta \\
 & + 2[\mu(i)\tau + \delta_i] \quad \text{with } i=1,2.
 \end{aligned} \quad (20)$$

Also $\Delta\mu = \mu_2 - \mu_1$. Figure 2 represents the in-phase injection with equal amplitudes. Here, the two solitons collide with each other at $\zeta = 0$. Figure 3 represents the off-phase injection with equal amplitudes. Here no soliton interaction takes place. Corresponding plots can be drawn for the case of unequal amplitudes also.

B. Constant pumping source case

Now let us construct the soliton solution for the constant pumping source case. For the constant pumping source case, $u(0) = \kappa = \kappa_+ + i\kappa_-$, which is taken as the seed solution. Hence,

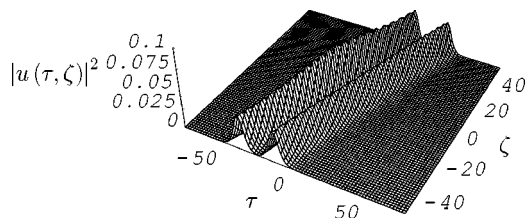


FIG. 3. Surface plot of the off-phase injection of the two soliton solution given by Eqs. (18), (19), and (20) when $g(\omega) = \delta(\omega - \omega_0)$, where the resonant frequency $\omega_0 = 0.5$.

$$\begin{aligned}
 \psi_{1\tau}(0) = & -i\lambda\psi_1(0) + \kappa\psi_2(0), \\
 \psi_{2\tau}(0) = & \kappa\psi_1(0) + i\lambda\psi_2(0).
 \end{aligned} \quad (21)$$

Hence from Eq. (21),

$$\begin{aligned}
 \psi_1(0) = & c_1(\zeta)\exp(-i\sqrt{\lambda^2 + |\kappa|^2}\tau), \\
 \psi_2(0) = & c_2(\zeta)\exp(i\sqrt{\lambda^2 + |\kappa|^2}\tau),
 \end{aligned} \quad (22)$$

where $c_i(\zeta)$ ($i=1,2$) are integration constants. Thus from Eq. (6), the corresponding wave functions are obtained as

$$\begin{aligned}
 \psi_1(0) = & c_1(0)\exp(\sqrt{A^2 + BC}\zeta - i\sqrt{\lambda^2 + |\kappa|^2}\tau), \\
 \psi_2(0) = & c_2(0)\exp[-(\sqrt{A^2 + BC}\zeta - i\sqrt{\lambda^2 + |\kappa|^2}\tau)].
 \end{aligned} \quad (23)$$

Hence the pseudospectral function $\Gamma(0)$ is given by

$$\Gamma(0) \equiv \frac{\psi_1(0)}{\psi_2(0)} = C(0)\exp[2(\sqrt{A^2 + BC}\zeta - i\sqrt{\lambda^2 + |\kappa|^2}\tau)], \quad (24)$$

where $C(0) \equiv c_1(0)/c_2(0)$. On substituting these in Eq. (11), the one-soliton solution is obtained as

$$\begin{aligned}
 u(\zeta, \tau) \equiv u(1) = & -(\kappa + 2\nu(1)\text{sech}\{2[S_R\zeta + M_I\tau + \nu(1)\Delta_1]\}) \\
 & \times \exp[2i(S_I\zeta - M_R\tau - \delta_1)],
 \end{aligned} \quad (25)$$

where

$$S_R = [\tfrac{1}{2}(D_R + \sqrt{D_R^2 + D_I^2})]^{1/2},$$

$$S_I = \frac{D_I}{2S_R},$$

$$M_R = [\tfrac{1}{2}(L_R + \sqrt{L_R^2 + L_I^2})]^{1/2},$$

$$M_I = \frac{L_I}{2M_R},$$

$$L_R = [\mu^2(1) - \nu^2(1) + |\kappa|^2],$$

$$L_I = 2\mu(1)\nu(1),$$

$$D_R = A_R^2 - A_I^2 + B_R C_R - B_I C_I,$$

$$D_I = 2A_R A_I + B_I C_R - B_R C_I, \quad (26)$$

and δ_1 and Δ_1 are integration phase constants. Also,

$$\begin{aligned}
 A_R = & 2\mu(1)\nu(1) - \left\langle \frac{\nu(1)}{2\{[\mu(1) + \omega]^2 + \nu^2(1)\}} \right\rangle \\
 & + 4\varepsilon\beta_1[3\mu^2(1)\nu(1) - \nu^3(1)] - 2\varepsilon\beta_1|\kappa|^2\nu(1),
 \end{aligned} \quad (27)$$

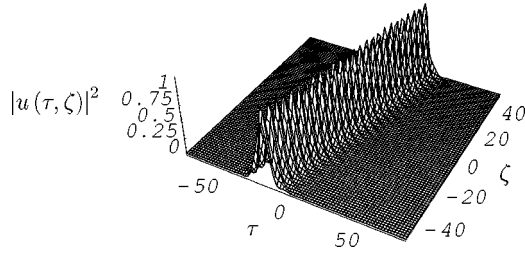


FIG. 4. Surface plot of the intensity of the soliton solution given by Eq. (25) when $g(\omega) = \delta(\omega - \omega_0)$ and $\kappa_+ = \kappa_- = 0.02$, where the resonant frequency $\omega_0 = 0.5$.

$$A_I = -[\mu^2(1) - \nu^2(1)] + \frac{1}{2}|\kappa|^2$$

$$- \left\langle \frac{\mu(1) + \omega}{2\{[\mu(1) + \omega]^2 + \nu^2(1)\}} \right\rangle + 4\varepsilon\beta_1$$

$$\times [3\mu(1)\nu^2(1) - \mu^3(1)] + 2\varepsilon\beta_1|\kappa|^2\mu(1),$$

$$B_R = \mu(1)\kappa_+ - \nu(1)\kappa_- + 4\varepsilon\beta_1\{\kappa_+[\mu^2(1) - \nu^2(1)]$$

$$- 2\mu(1)\nu(1)\kappa_-\} - 2\varepsilon\beta_1|\kappa|^2\kappa_+,$$

$$B_I = \mu(1)\kappa_- + \nu(1)\kappa_+ + 4\varepsilon\beta_1\{\kappa_-[\mu^2(1) - \nu^2(1)]$$

$$- 2\mu(1)\nu(1)\kappa_+\} - 2\varepsilon\beta_1|\kappa|^2\kappa_-,$$

$$C_R = -\mu(1)\kappa_+ - \nu(1)\kappa_- - 4\varepsilon\beta_1\{\kappa_+[\mu^2(1) - \nu^2(1)]$$

$$+ 2\mu(1)\nu(1)\kappa_-\} + 2\varepsilon\beta_1|\kappa|^2\kappa_+,$$

$$C_I = -\mu(1)\kappa_- - \nu(1)\kappa_+ + 4\varepsilon\beta_1\{\kappa_-[\mu^2(1) - \nu^2(1)]$$

$$- 2\mu(1)\nu(1)\kappa_+\} - 2\varepsilon\beta_1|\kappa|^2\kappa_-,$$

$$\kappa = \kappa_+ + i\kappa_-.$$

Figure 4 shows the surface plot for the intensity $|u(\zeta, \tau)|^2$ when $g(\omega) = \delta(\omega - \omega_0)$. From the figure, it is clear that $|u(\zeta, \tau)|^2$ has a constant value equal to $|\kappa|^2$ instead of zero when $\tau \rightarrow \pm\infty$. It can also be seen that when $\kappa \rightarrow 0$, Eq. (25) reduces to Eq. (14). Following a similar procedure as in case (i), the expressions for $p(\zeta, \tau)$ and $\eta(\zeta, \tau)$ pertaining to the soliton solution given by Eq. (25) can be readily obtained from the master equation (3).

Once again on using the recurrence relations given by Eq. (11), the two-soliton solution for Eq. (3) is obtained and is of the form

$$u(2) \equiv u_2(\zeta, \tau) = \frac{\kappa D(\zeta, \tau) + N(\zeta, \tau)}{D(\zeta, \tau)}, \quad (28)$$

where $N(\zeta, \tau)$ and $D(\zeta, \tau)$ have the same form as Eq. (19). In this case, ξ_i and χ_i ($i=1,2$) have the following expressions:

$$\xi_1 = 2[S_R\zeta + M_I\tau + \nu(1)\Delta_1],$$

$$\xi_2 = 2[S_{2R}\zeta + M_{2I}\tau + \nu(2)\Delta_2],$$

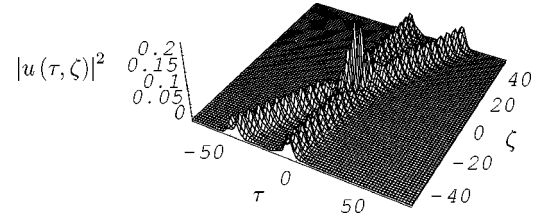


FIG. 5. Surface plot of the in-phase injection of the two soliton solution given by Eqs.(28), (29), and (30) when $g(\omega) = \delta(\omega - \omega_0)$ and $\kappa_+ = \kappa_- = 0.02$, where the resonant frequency $\omega_0 = 0.5$.

$$\chi_1 = 2(-S_I\zeta + M_R\tau + \delta_1),$$

$$\chi_2 = 2(-S_{2I}\zeta + M_{2R}\tau + \delta_2), \quad (29)$$

where S_R , S_I , M_R , and M_I are given by Eq. (26). Now

$$S_{2R} = \left[\frac{1}{2}(D_{2R} + \sqrt{D_{2R}^2 + D_{2I}^2}) \right]^{1/2}, \quad (30)$$

$$S_{2I} = \frac{D_{2I}}{2S_{2R}},$$

$$M_{2R} = \left[\frac{1}{2}(L_{2R} + \sqrt{L_{2R}^2 + L_{2I}^2}) \right]^{1/2},$$

$$M_{2I} = \frac{L_{2I}}{2M_{2R}},$$

where

$$L_{2R} = [\mu^2(2) - \nu^2(2) + |\kappa|^2],$$

$$L_{2I} = 2\mu(2)\nu(2),$$

$$D_{2R} = A_{2R}^2 - A_{2I}^2 + B_{2R}C_{2R} - B_{2I}C_{2I},$$

$$D_{2I} = 2A_{2R}A_{2I} + B_{2I}C_{2R} - B_{2R}C_{2I},$$

$$A_{2R} = 2\mu(2)\nu(2) - \left\langle \frac{\nu(2)}{2\{[\mu(2) + \omega]^2 + \nu^2(2)\}} \right\rangle$$

$$+ 4\varepsilon\beta_1[3\mu^2(2)\nu(2) - \nu^3(2)] - 2\varepsilon\beta_1|\kappa|^2\nu(2),$$

$$A_{2I} = -[\mu^2(2) - \nu^2(2)] + \frac{1}{2}|\kappa|^2$$

$$- \left\langle \frac{\mu(2) + \omega}{2\{[\mu(2) + \omega]^2 + \nu^2(2)\}} \right\rangle + 4\varepsilon\beta_1[3\mu(2)\nu^2(2)$$

$$- \mu^3(2)] + 2\varepsilon\beta_1|\kappa|^2\mu(2),$$

$$B_{2R} = \mu(2)\kappa_+ - \nu(2)\kappa_- + 4\varepsilon\beta_1\{\kappa_+[\mu^2(2) - \nu^2(2)]$$

$$- 2\mu(2)\nu(2)\kappa_-\} - 2\varepsilon\beta_1|\kappa|^2\kappa_+,$$

$$B_{2I} = \mu(2)\kappa_- + \nu(2)\kappa_+ + 4\varepsilon\beta_1\{\kappa_-[\mu^2(2) - \nu^2(2)]$$

$$- 2\mu(2)\nu(2)\kappa_+\} - 2\varepsilon\beta_1|\kappa|^2\kappa_-,$$

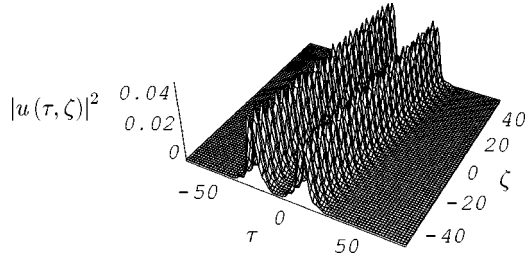


FIG. 6. Surface plot of the off-phase injection of the two soliton solution given by Eqs. (28), (29), and (30) when $g(\omega) = \delta(\omega - \omega_0)$ and $\kappa_+ = \kappa_- = 0.01$, where the resonant frequency $\omega_0 = 0.5$.

$$C_{2R} = -\mu(2)\kappa_+ - \nu(2)\kappa_- - 4\varepsilon\beta_1\{\kappa_+[\mu^2(2) - \nu^2(2)] + 2\mu(2)\nu(2)\kappa_-\} + 2\varepsilon\beta_1|\kappa|^2\kappa_+,$$

$$C_{2I} = -\mu(2)\kappa_- - \nu(2)\kappa_+ + 4\varepsilon\beta_1\{\kappa_-[\mu^2(2) - \nu^2(2)] - 2\mu(2)\nu(2)\kappa_+\} - 2\varepsilon\beta_1|\kappa|^2\kappa_-.$$

Figure 5 accounts for the in-phase injection between two solitons for equal amplitudes for the case when $\kappa_+ = \kappa_- = 0.02$ and when the central frequency $\omega_0 = 0.05$, while Fig. 6 portrays the off-phase injection. From the above mentioned figures, it is clear that $|u(\zeta, \tau)|^2$ has a constant value equal to $|\kappa|^2$ instead of zero when $\tau \rightarrow \pm\infty$. It can also be seen that when $\kappa \rightarrow 0$, Eq. (28) reduces to Eq. (18).

IV. CONCLUSIONS

This paper concerns the coherent soliton pulse interaction in an erbium doped fiber system associated with the higher-order dispersion, self-steepening, and self-induced transparency effects. Using auto-Bäcklund-transformation, one- and two-soliton solutions with and without the continuous wave background have been generated. As usual, it is observed that there is an exact balancing between higher-order perturbation terms present in Eq. (3) and self-induced transparency effects. Next, the soliton solution when the erbium-doped fiber system is driven by a constant pumping source is considered. In this case, the soliton solution will have a constant value equal to that of pumping source even at infinity, a phenomenon which differs from the case where the soliton solution asymptotically decreases to zero at infinity. This is depicted as the soliton in a continuous wave background. The interaction scenario is also studied in detail for both the cases. Future work includes a study of the influence of TOD, SS, and SRS effects on the interaction scenario for the HNLS-MB system with continuous wave background.

ACKNOWLEDGMENTS

V.C.K. wishes to acknowledge IUCAA, Pune for support. K.P. wishes to thank DST and CSIR, Government of India, for financial support through research projects.

-
- [1] G.P. Agrawal, *Nonlinear Fiber Optics* (Academic Press, San Diego, 2001); *Applications of Nonlinear Fiber Optics* (Academic Press, San Diego, 2001).
- [2] Y.S. Kivshar and G.P. Agrawal, *Optical Solitons—From Fibers to Photonic Crystals* (Academic Press, San Diego, 2002).
- [3] S.L. McCall and E.L. Hahn, *Phys. Rev. Lett.* **18**, 908 (1967); *Phys. Rev.* **183**, 457 (1969).
- [4] G.L. Lamb, Jr., *Rev. Mod. Phys.* **43**, 99 (1971); *Phys. Rev. A* **9**, 422 (1974).
- [5] V.B. Matveev and M.A. Salle, *Darboux Transformations and Solitons* (Springer, Berlin, 1991).
- [6] Y. Kodama and A. Hasegawa, *IEEE J. Quantum Electron.* **23**, 510 (1987).
- [7] A.I. Maimistov and E.A. Manykin, *Sov. Phys. JETP* **58**, 685 (1983).
- [8] A.I. Maimistov, A.M. Basharov, S.O. Elyutin, and Yu M. Sklyarov, *Phys. Rep.* **191**, 1 (1990).
- [9] A.I. Maimistov, *Opt. Commun.* **94**, 33 (1992).
- [10] A.I. Maimistov and A.M. Basharov, *Nonlinear Optical Waves* (Kluwer Academic Publishers, Dordrecht, 1999).
- [11] Y. Kodama, *Phys. Lett. A* **107**, 245 (1985).
- [12] N. Sasa and J. Satsuma, *J. Phys. Soc. Jpn.* **60**, 409 (1991).
- [13] Y. Kodama, *J. Stat. Phys.* **39**, 597 (1985).
- [14] R. Hirota, *J. Math. Phys.* **14**, 805 (1973).
- [15] Q-Han Park and R.W. Boyd, *Phys. Rev. Lett.* **86**, 2774 (2001).
- [16] D.P. Caetano, S.B. Cavalcanti, and J.M. Hickmann, *Phys. Rev. E* **65**, 036617 (2002).
- [17] M. Nakazawa and K. Kurokawa, *Electron. Lett.* **27**, 1369 (1991).
- [18] K. Kurokawa and M. Nakazawa, *Electron. Lett.* **27**, 1765 (1991).
- [19] E.V. Doktorov and R.V. Vlasov, *Opt. Acta* **30**, 223 (1983).
- [20] E.V. Doktorov and R.V. Vlasov, *J. Phys. Soc. Jpn.* **65**, 876 (1996).
- [21] K. Porsezian and K. Nakkeeran, *J. Mod. Opt.* **42**, 1953 (1995).
- [22] S. Kakei and J. Satsuma, *J. Phys. Soc. Jpn.* **63**, 885 (1994).
- [23] K. Porsezian and K. Nakkeeran, *Phys. Rev. Lett.* **74**, 2941 (1995).
- [24] K. Nakkeeran and K. Porsezian, *J. Phys. A* **28**, 3817 (1995).